# Optical Fiber Based Distributed Mechanical Vibration Sensing

**Vít Novotný [1*], Petr Sysel [2] Aleš Prokeš [3], Pavel Hanák [4], Karel Slavíček [5] and Jiří Přinosil [6]**

[1]   Faculty of Business and Management, Brno University of Technology, novotnyv@fbm.vutbr.cz,
[2,3,4,5,6] Faculty of Electrical Engineering and Communication, Brno University of Technology, sys-
      el@feec.vutbr.cz, prokes@feec.vutbr.cz, hanakp@feec.vutbr.cz, slavicekkarel@feec.vutbr.cz,
      prinosil@feec.vutbr.cz

**Abstract:** The distributed long-range sensing system using the standard telecommunication single-mode optical fiber in a function of a distributed sensor for sensing of mechanical vibrations is described. Various events generating vibrations such as walking or running person, moving cars, trains and others can be detected, localized and classified. The sensor and related sensing system components were designed and constructed and the system was tested both in the laboratory and in the real situation with 88 km telecom optical link, and the results are presented.

**Keywords:** distributed fiber optic sensor, vibration sensor, mechanical vibrations, φ-OTDR

## 1. Introduction

Optical fibers are used mainly in the area of telecommunications where the optical fibers can transport data at bit rates in the range of terabits per second each. Optical fibers spreads almost across whole network infrastructure, i.e. not only in the area of WANs but they are implemented also in data centers, within enterprise networks, in complex telecommunication distribution nodes, in and also in access data networks ("first-mile") called as FTTx technologies (Fiber-To-The x = given point between customer and provider central office, e.g. H = Home) mainly in the form of passive optical networks (PONs), [1].

Optical fiber applications as sensors are another very attractive area. Fiber construction, the principle of its operation (total reflection) and the form of signal (light) makes the transmission of data very safe, reliable and resistant to many sources of disturbances but nevertheless the fiber parameters are partially sensitive to ambient conditions, [2], such as temperature, strain, vibrations or strong ambient electromagnetic field and this has impact on optical signal travelling through a fiber. These facts are used for sensing application, [2]. Chemical and biochemical sensors using fibers are also available.

Majority of sensor applications are point sensors or quasi-distributed but more and more applications using optical fiber in fully distributed manner are investigated where not only physical quantity value can be measured but also the location information is provided so that long ranges of fiber length can be used for multiple simultaneous measurements.

Distributed sensors are used to measure quantities such as temperature, strain, mechanical vibrations, solutions are used to guard pipelines, rails, frontiers, territories, etc., [3, 4, 5, 6].

*1.1. Sensing capabilities of fibers*

Two groups of fiber sensors are defined, [2]:
1.      extrinsic (hybrid) fiber optic sensors,
2.      intrinsic fiber optic sensors.

Extrinsic sensors are sensors where sensing point is located outside the fiber itself while the second group of sensors uses optical fiber material as a sensory medium. Fiber sensors can be used as:

- a point sensor where there is only one point of sensing or where the quantity is spread equally along the fiber, or
- a distributed sensor where the measured quantity has local influence and the used measurement method is capable to localize it, so that the fiber trace can represent hundreds or thousands of sensors.

A general scheme of a sensor using optical fibers as a sensing element is shown in **Figure 1**:
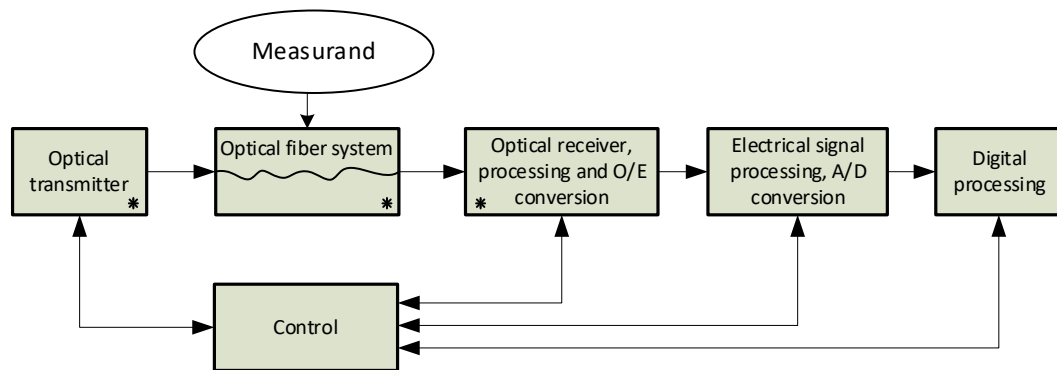
**Figure 1.** General architecture of modern optical fiber-based sensing system.

An optical transmitter contains a light source - a laser that is the most frequently used type, and in majority applications also a modulator, amplifiers, filters and other components are present to generate a special form of the light signal with appropriate power level and limited spectrum. In most cases the monochromatic and very stable, i.e. a highly coherent light source is required to obtain high sensor sensitivity and required accuracy.

The optic fiber system includes one or more fiber segments and the other components, such as optical splitters, couplers, isolators, circulators and in some schemes also polarization controllers, polarization splitters, prisms, lenses and mirrors may be a part of it. The block of optical reception, processing and o/e conversion may include optical preamp, an optical filter and/or a block for coherent detection that may precede an o/e converter. Optical detectors change a stream of photons into an electrical signal, i.e. current or voltage that is processed by conventional electronics before A/D conversion. PIN and avalanche photodiodes are the most common photodetectors used for sensing purposes. The most important parameters of the photodiodes are the optical power dynamic range, the spectral sensitivity and the quantum efficiency, the bandwidth, the noise level and the voltage and temperature dependencies of parasitic effects like the junction capacitance and the dark current. Majority of these parameters are dependent on a circuit scheme and on the ambient temperature. The temperature has negative impact mainly on the dark current. If the temperature increases approximately by 8 °C, the dark current doubles its value, [7]. Dynamic behavior (response time) of the photodiode is dependent on several factors, on the size of photoelement, the bias voltage and especially on the wavelength for which the photodiode was designed - the shorter wavelength, the thinner depletion region has to be implemented in photodiode and faster response is reached. The shorter response time can be reached by narrowing the silicon layer at the cost of lower quantum efficiency and of the overall sensitivity. Low noise amplifier (LNA) is also a necessary part of the optical detector. The coherent heterodyne detection scheme contains a balanced photodetector with couple of matched photodiodes.

The A/D converter with antialiasing filter is the input part of the digital signal processing block. The sampling frequency should fulfil Nyquist–Shannon sampling theorem and the dynamic range (a number of bits per sample) should correspond to the maximum signal-to-noise ratio. To measure the signal, whose dynamics is 70 dB, the A/D converter with 12-bit resolution at least is required.

### 1.2. Fiber sensing principles

There is a number of principles using an optical fiber that have been designed, tested and used for sensing purposes during the decades by many scientist and engineers working in this area of research [2]. The first group of methods is based on the simplest effect, i.e. light intensity change. These sensors are either based on violation of total reflection principle of light propagation along the fiber (pressure or position sensors based on fiber microbending) or they belong to the extrinsic sensors when external light propagation parameters change when the light leaves the fiber, reflects from the reflector and returns back to the detector. A big group of sensors uses a light interferometry principle [8]. This group of sensors is based on the result of light interference. They use phase differences between light beams that travel through interferometer arms and then meet each other and interfere. The proper function requires interfering beams to be highly coherent and therefore the difference of arm lengths must be lower than the coherence length of the laser source. Fabry-Pérot, Mach-Zehnder, Michelson, and Sagnac are the most known interferometer principles, [8]. The interferometric methods are very sensitive but if used as intrinsic sensor for vibration sensing their results do not give information about the location.

### 1.3. Distributed optical fiber vibration sensors

Distributed optical fiber vibration sensors have capability of mechanical vibrations sensing in its vicinity in distributed manner, i.e. it can detect and localize many events simultaneously located at different points along the sensing fiber. Many techniques and measurement methods and schemes were proposed during last two decades, [3 - 24]. The most common measurement scheme is based on the analysis of Rayleigh backscattered signal from interrogating pulses sent to the fiber, similar to the reflectometry principle used in OTDR, see Figure 2, but the sensing principle is different and based on the changes of interference patterns among discrete scattering centers within half of the optical pulse width, [10, 13]. Other effects can be used for distributed sensing of a temperature or a strain, e.g. Brillouin or Raman ones, [9, 10].
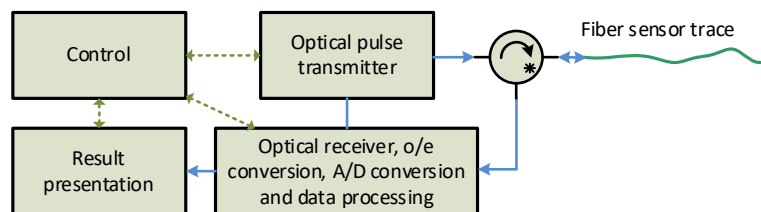
**Figure 2**. Block structure of the distributed fiber sensor utilizing signal backscattering principle.

To reach high sensitivity the highly coherent lasers are required. Narrow and highly coherent optical pulses are regularly sent to the fiber and backscattered optical signal is received at the same sensing fiber end. The sensing fiber may be exposed to mechanical vibrations, which change the sensing fiber parameters (length, width and refracting index) and so do the parameters of a propagating optical signal. Received signal is processed and a huge amount of information from it can be obtained about the fiber. Obtained data is used firstly for detection of events and in positive case the event sources can be localized and also classified. "Time-of-flight" technique is used for localization. Sophisticated signal processing techniques are necessary if event classification is required.
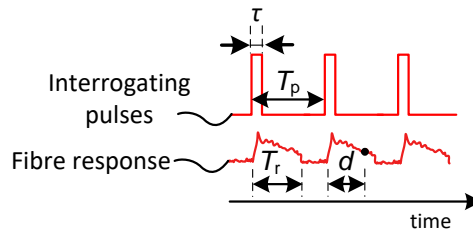
**Figure 3**. Interrogating optical pulse sequence course, properties and the fiber backscattering responses.

A portion of this scattered signal is re-captured by the fiber and part of it is being spread back to the fiber origin, see **Figure 3**. The pulse width $\tau$ limits distributed sensor spatial resolution $R$ that can be calculated as:

$$R = \frac{\tau v_g}{2},\qquad(1)$$

where $v_g$ is the light group velocity in the fiber core. The equation (1) clearly shows that the sensor spatial resolution can be increased by narrowing the interrogation pulses. Nevertheless, the narrower pulse at the same power carries less energy and therefore shorter sensing ranges are usually reached because of the limited detector sensitivity and a noise presence. Fast modulators or other techniques are required to generate nanosecond or shorter pulses. Acousto-optic modulators (AOM) modulators cannot be used as their rise/fall times are in tens ns range. Increasing the pulse power to carry more energy may cause nonlinear effects in the fiber and decreasing the signal to noise ratio.

**Figure 4** depicts a pulse sequence sent to the sensing fiber and related backscattering responses to them. Provided the pulse light carrier is unchanged the pulse period $T_P$ has to be longer than the fiber backscattering response $T_r$, otherwise the responses from the neighbor pulses would overlap and the information from the fiber will be partially lost. For example, when the sensing fiber is 10 km long, the pulse period has to be longer than 100 μs. A solution how to overcome this restriction was proposed in [25] but we have not realized it yet.
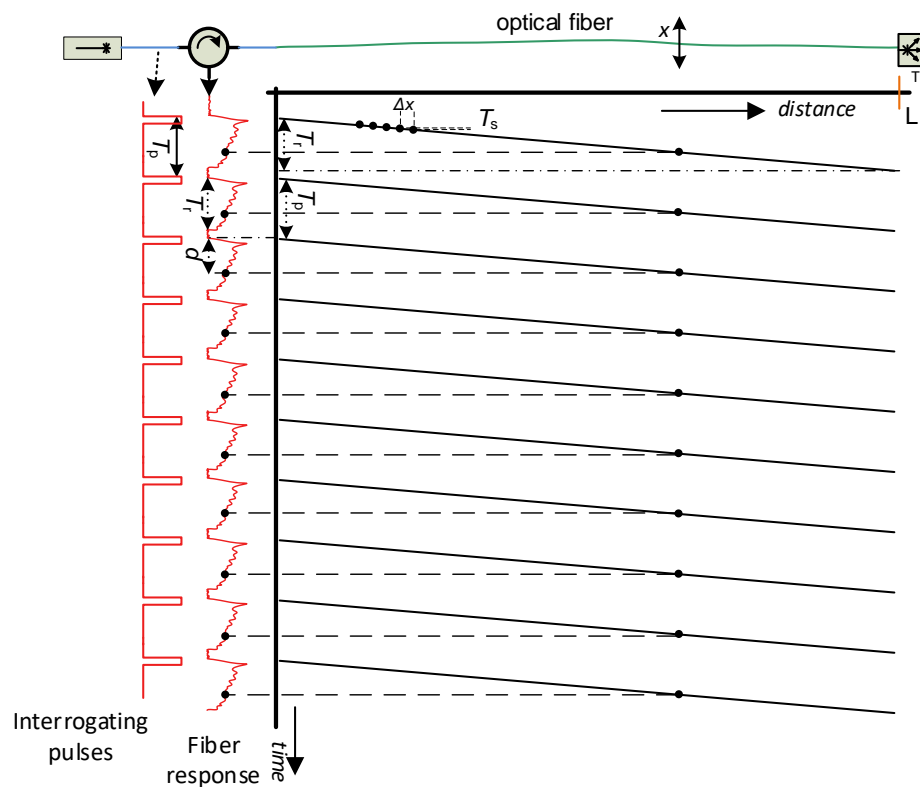
**Figure 4**. Time-spatial fiber backscattering response on the sequence of optical interrogation pulses.

The latency $d$ between time instances of light pulse transmissions and the instance of the response sample reception (see **Figure 4**) can be used to calculate the location $x$ of an event,

$$x \approx \frac{d * v_{\mathrm{g}}}{2}.$$

(2)

Usually the distance $x$ at the fiber is impractical for a customer and hence an event geographical location should be found. This requires knowledge of sensing cable laying as accurately as possible. Then the event geographical coordinates can be calculated as an approximation between two closest points on the fiber whose precise geographical locations are stored in a database.

Standard course of the fiber backscattering response based on the technique described above after o/e conversion is shown in **Figure 5**. The fast signal attenuation and its high fluctuations can be indicated in the figure. The rapid signal attenuation is caused by double attenuation both of interrogating pulses in forward direction and of backscattered signal in backward direction. Backscattered signal fluctuations come from the usage of a highly coherent laser source, random locations of scattering centers within the sensing fiber and from random phase of scattered signal contributions generated at scattering centers that interfere within the half pulse width, [10]. Due to this effect (destructive phase interference) and also due to the mutually almost orthogonal polarizations of a local oscillator and received backscattered signal (in the case of coherent detection, see below) the signal level falls close to zero level at many time instants and this deteriorates the sensor sensitivity at corresponding locations along the sensing fiber.
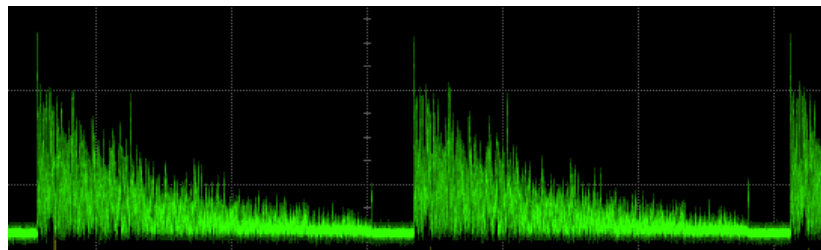
**Figure 5**. Typical fiber response to narrow spectral linewidth interrogating pulses

Two basic schemes are used for backscattered signal reception – direct detection and coherent heterodyne detection, which can be seen in **Figure 6** and **Figure 7**.
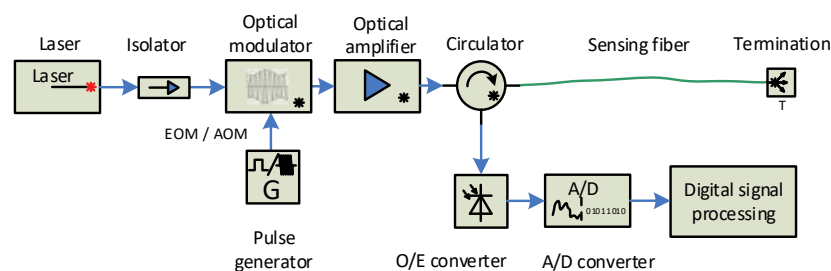
**Figure 6**. Direct detection scheme
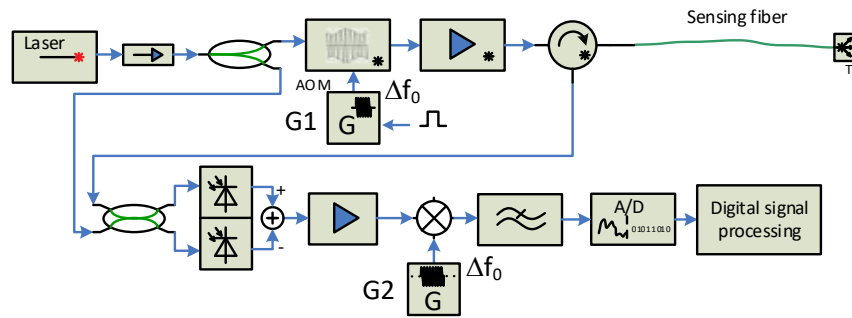
**Figure 7**. Coherent heterodyne detection scheme

Both schemes contain a laser source protected by an optical isolator, followed by an optical amplifier and an optical circulator in the forward branch of the sensor, and an o/e convertor, an acquisition board and a computer unit for the digital processing in the reception arm. The main difference of the coherent detection scheme consists in the application of a local oscillator signal mostly derived from the main laser, its mixing with backscattered signal and in the usage of the balanced o/e converter in which the beat signal amplification process occurs. When heterodyne version is used, an analog mixer to obtain baseband signal is required.

Direct detection scheme has lower complexity than coherent one but it has a number of issues described in [13] that limit its performance. As described briefly above the coherent detection technique consists in mixing of backscattered signal with optical local oscillator and in a balanced o/e conversion. The strong local oscillator signal is mixed with a weak backscattered signal in a 50/50 coupler and converted to an electrical signal in a balanced photodetector. The beat signal generates in the balanced photodetector a current given by the formula (3) [10]

$$I_1 - I_2 = 2R\sqrt{P_S(t)P_L}\,\sin\left[\omega_{AOM}t + \theta_S(t) - \theta_L\right],\tag{3}$$

which shows the main principle of the weak fiber response amplification, $R$ is the convertor responsivity (A/W), $P_S$ is the power of received signal, $P_L$ is the power of the local oscillator, $\omega_{AOM}$ is the angle frequency of rf pulses driving the AOM modulator and $\theta_S$ and $\theta_L$ are phases of the signal and of the local oscillator respectively. This method improves sensor sensitivity and provides higher dynamic range. The cost for these advantages is that an ultra-narrow spectrum light source (laser) with high stability is required. Its spectrum line width has to be in the order of units of kHz or better, thus the laser is usually the most expensive component of such systems.

The sensor performance can be partially improved by adding an optical bandpass filter behind the optical power amplifier to suppress the ASE noise generated by it. Additional improvement can be reached by adding of an optical amplifier followed by an optical filter to the reception path behind the third port of the circulator. As the generators G1 and G2 are not perfectly synchronized and stable, an additional signal deterioration may occur. Small improvement can be reached by using one harmonic generator with pulse shaper and power amplifier to drive the AOM as shown in **Figure 8**. The rf signal generator driving the AOM is not perfectly stable too. As the fiber response duration is much longer than radio pulse sent to the AOM modulator, the generator phase and/or frequency may change and that causes a partial distortion of the signal coming from larger distances of the sensing fiber, i.e. with larger latency.
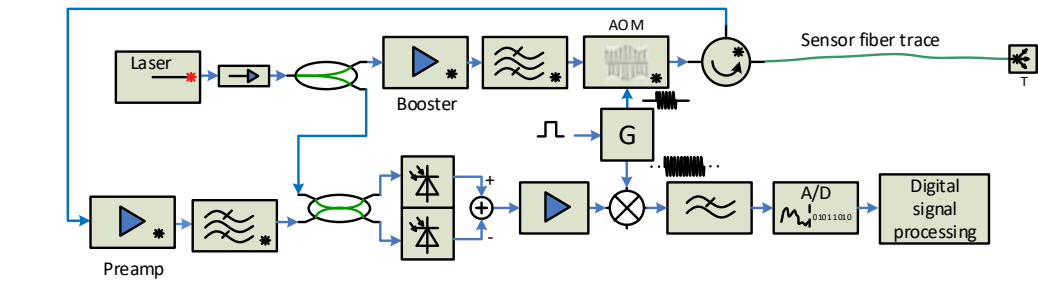
**Figure 8**. Coherent detection scheme with a single RF signal source

Provided the carrier of the beat signal can be recovered from the received signal, the issue can be solved by the self-mixing technique described in [20]. The result scheme is shown in **Figure 9**. Electrical bandpass filter behind the o/e balanced converter allows only the beat signal to pass, and the following voltage-controlled gain amplifier (VGA) amplifies and equalizes the fiber response characteristics. VGA output signal is splitted into two branches then and one enters the carrier recovery unit before mixing process.
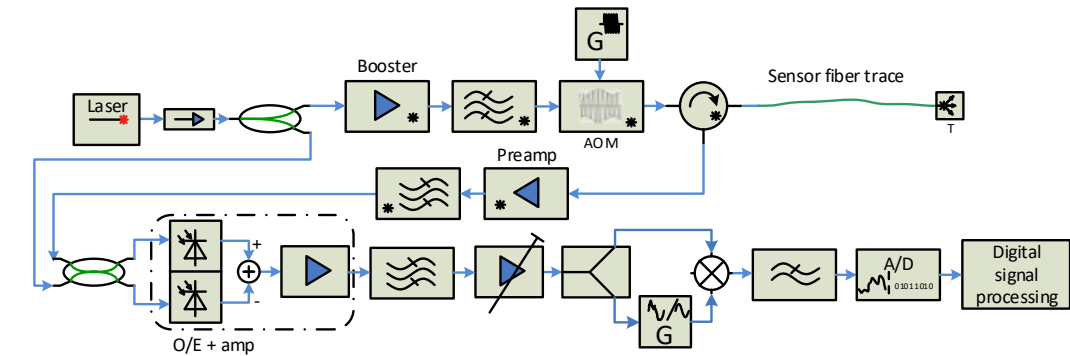
**Figure 9**. Final sensor unit scheme used of the test-bed.

As the sensor components like the laser, the optical amplifiers, the modulator and o/e converter are quite expensive, it can be valuable to have a scheme, which uses at least some of these elements more efficiently. This can be reached by the design of scheme with more sensing branches consisting of several sensing fibers and of several reception and processing chains.

**Figure 10** shows two-trace scheme with two sensing fibers and two reception and processing chains.
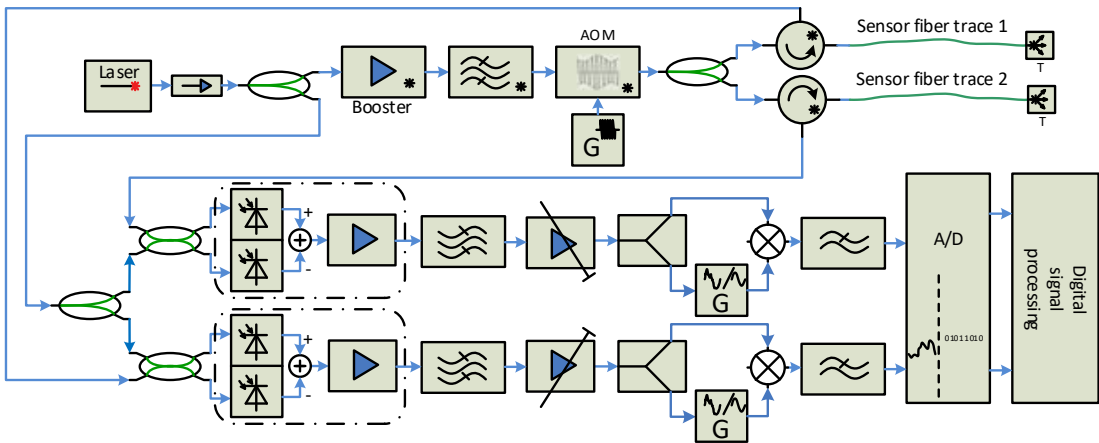
**Figure 10**. Two-trace sensor unit

The pulse signal generated by the AOM enters 1x2 splitter and its outputs are connected via circulators into two sensing arms. The backscattered signals from each fiber is separately processed by the coherent heterodyne detectors and converted to digital form for digital processing.

## 2. Experimental measurements

To test the principles mentioned above several experimental test-beds were designed and realized. The direct detection architecture was found less sensitive than coherent one and thus the coherent heterodyne detection system was selected and the result design is based on the scheme shown in **Figure 7**.

The first version of interrogation unit we realized and tested was in 2015 and results were presented in [26]. Later we designed a new version of sensor probe according to the scheme from **Figure 9** that was constructed in 2018. We used ultra narrow laser (10 kHz linewidth) at 1550 nm wavelength to minimize the signal attenuation (both interrogating pulse and backscattered signal) along the fiber. The pulses are generated by acousto-optic modulator (AOM), which in addition to modulation process with high extinction ratio (> 50 dB) shifts the spectrum of optical signal in order of tens MHz, [15, 16]. We used AOM with 110 MHz frequency shift. The pulse width can be selected in the range 100 ns - 1 µs. The pulse width corresponds to a spatial resolution that is in a range 10 - 100 m. Generated pulses are amplified by EDFA booster, filtered by an optical bandpass filter and sent via the circulator to the fiber. The backscattered optical signal from the fiber returns via the optical circulator and enters the EDFA preamplifier and after filtering is mixed with optical local oscillator (OLO) signal generated by the laser in 50/50 coupler. Result signal is converted to the electrical form by a balanced o/e converter containing PIN photodiode and transimpedance amplifier. The electrical signal is again amplified and equalized and then splitted into two branches. The signal of one is used to recover the beat carrier, i.e. 110 MHz signal, which is then mixed the second branch signal. High frequency components (above 10 MHz) of the mixer output are filtered out and the result signal is converted to the digital form by A/D converter with sampling frequency 50 MSPS. Obtained data is processed by additional filtering and averaging techniques. The system was constructed and tested in a laboratory (fiber coils of length 20 and 50 km) first and later connected to a real optical telecom link.
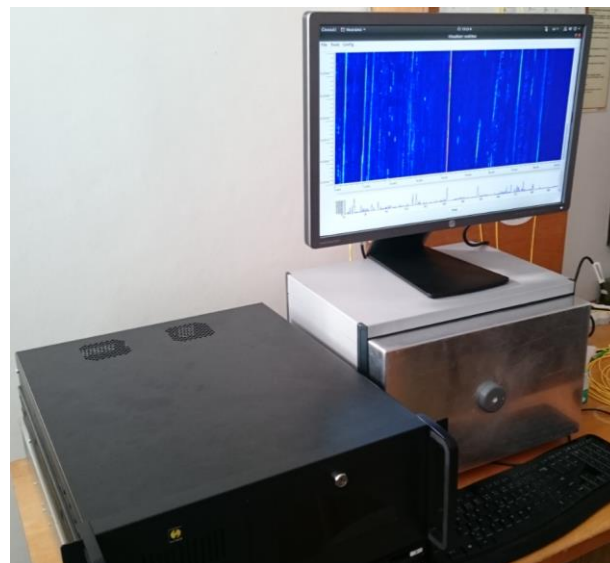
**Figure 11**. The single fiber sensing unit testing in a real enviroment

Sensing optical fiber was a dark fiber in a standard telecommunication optic cable with total length of 88 km.
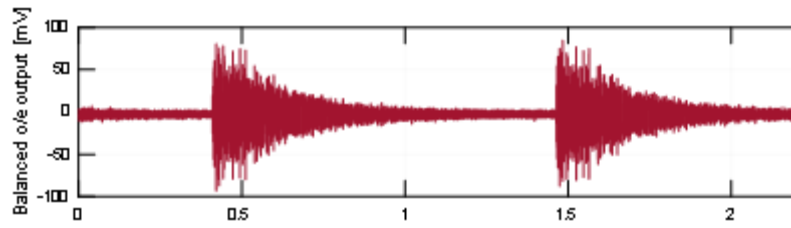
**Figure 12**. The beat signal at the output of balanced o/e converter

Small segment of the output signal from the o/e converter is shown in **Figure 13**. What we are interested in, is the envelope of the result beat signal, which will be obtained after mixing with the carrier frequency and lowpass as described above. We recovered the carrier from the received beat signal as depicted in **Figure 9**.
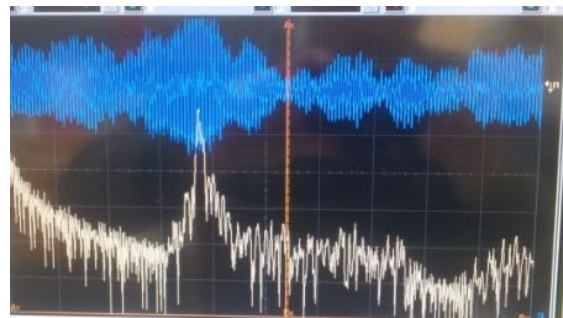
**Figure 13**. Signal detail after an o/e conversion and its spectrum – coherent heterodyne detection system.

After low-pass filtering the signal shown in **Figure 14** is obtained.
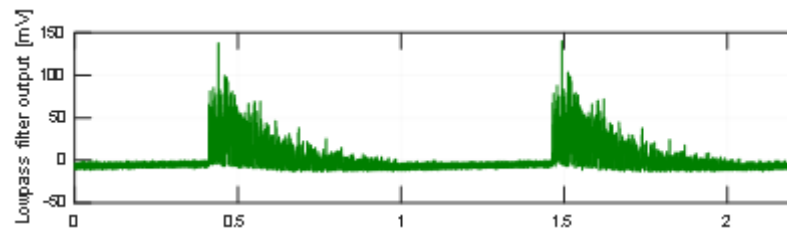
**Figure 14**. Signal after demodulation without equalization (almost 2 periods)

Due to the exponential attenuation of the fiber response the signal level is quite weak from large distances. Therefore a fiber response equalization was proposed and implemented. To equalize the response the beat signal was amplified by the logarithmic variable gain amplifier (VGA) whose gain was controlled by the sawtooth shaped signal synchronized with the pulse generation, see **Figure 15**.
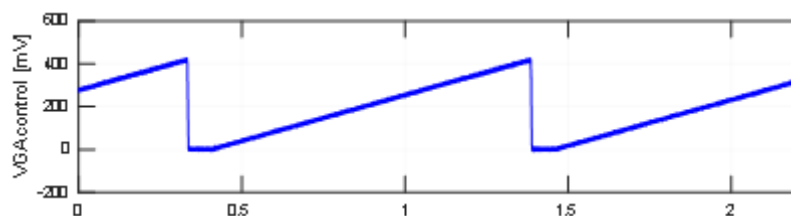
**Figure 15**. VGA control voltage

After equalization and demodulation processes and lowpass filtering (see **Figure 16**) the signal is converted to the digital form for digital processing.
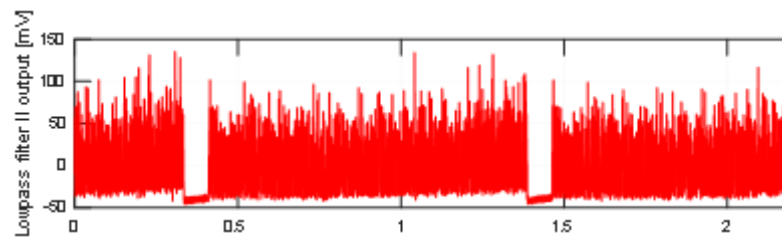
**Figure 16**. Signal after demodulation and equalization

To display the situation along the fiber and during a time period a software was designed to arrange the fiber responses in two-dimensional matrix with the color representing signal level. Such signal representation is called "waterfall" in the raw form is obtained. Two-dimensional signal displays information along the fiber (horizontal axis) and in time (vertical axis, latest response is at the top), see **Figure 17** (only a narrow part of waterfall in the horizontal direction with a static event occurrence within the interval of 7 seconds is shown). The event caused by the hammer strokes on a rail was detected at the distance of 74.4 km along the fiber.
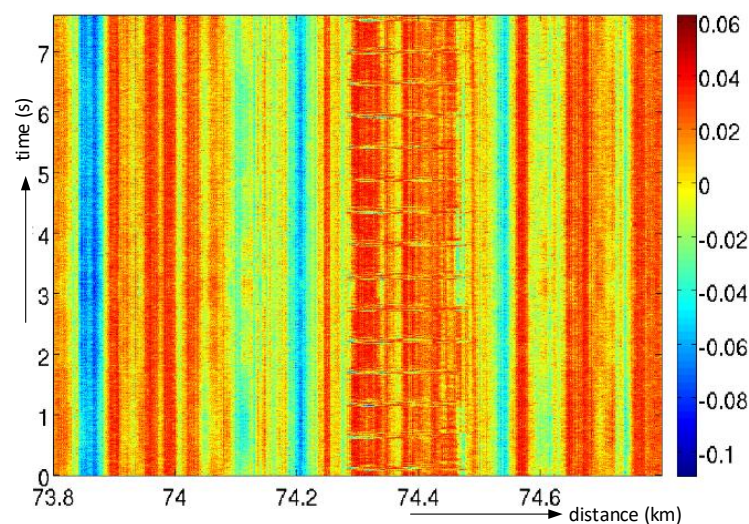
**Figure 17**. A "waterfall" of raw captured data.

Using FIR filtering along the time axis the vibration events along the fiber can be emphasised while the quiet areas are cleaned as shown in **Figure 18**.
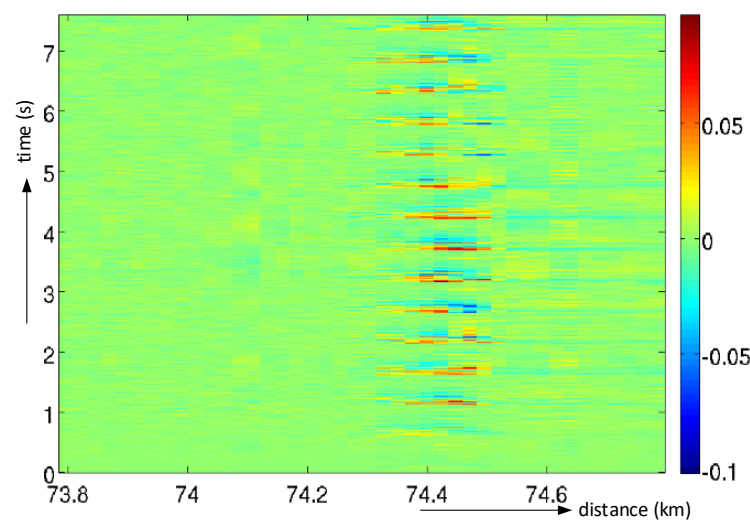
**Figure 18**. An example of a "waterfall" with a detected event after filtering

The corresponding time-domain course of the signal (hammer strokes) from the single point in the fiber is shown in **Figure 19**.
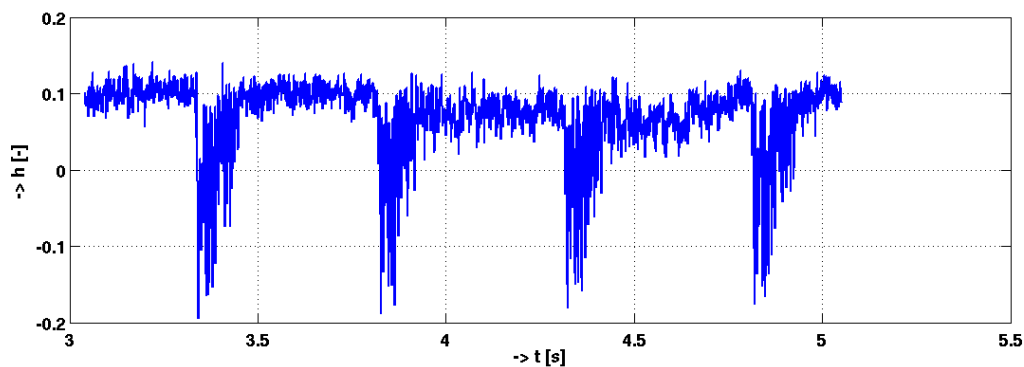
**Figure 19**. Time-domain signal amplitude evolution from the event location – hammer strokes

The waterfall with non-static events along the complete sensing fiber (88 km long) is depicted in **Figure 20**. Due to the distributed sensing principle several simultaneous events can be detected and separately processed.
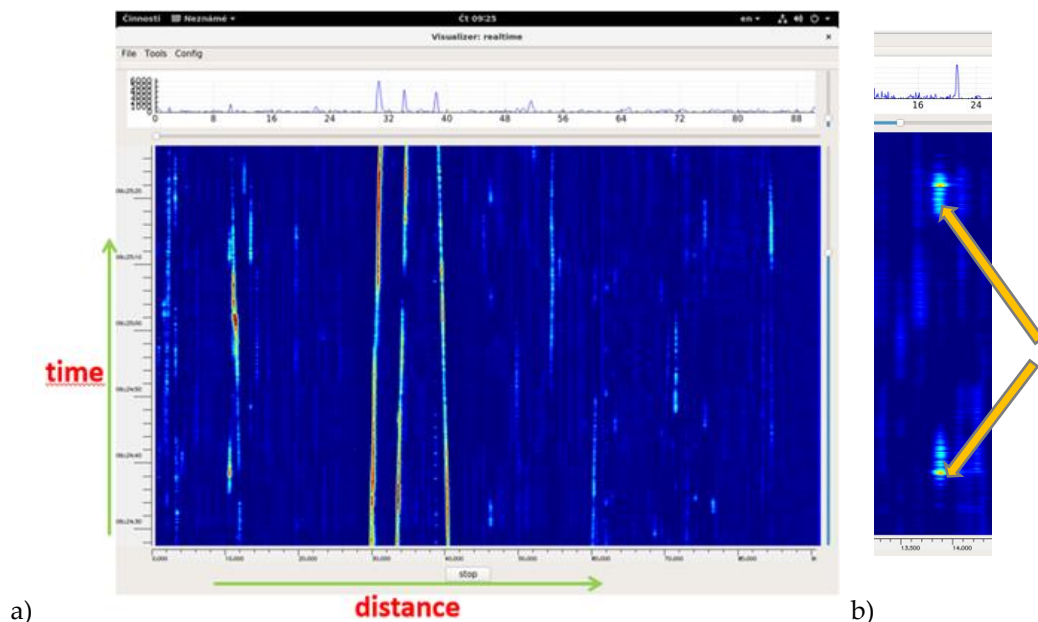
**Figure 20**. Waterfall of of the occurrence of a) multiple simultaneous events - "waterfall", b) a vehicle passing a rail crossing

The speed of vibration source movement can be derived from the slope of the track in the waterfall, see **Figure 21**. There can be troubles to establish the speed precisely. First, we need to determine the reference points on the fiber at particular time instants. This can be a problem both when the sources produce too strong or too weak vibrations, compare **Figure 21** and **Figure 20**a). In the first case the track is wide and its width changes, and in the second case the track vanishes at some locations, so that the extrapolation method is required. The sensing fiber along the railways or roads bends and rolls so it can cause that calculated distance segments within the time periods can differ significantly. After the locations at different time instants along the fiber are obtained from the detection process, the geographical coordinates have to be determined. That is why the precise geolocation information about the sensing cable laying is required.
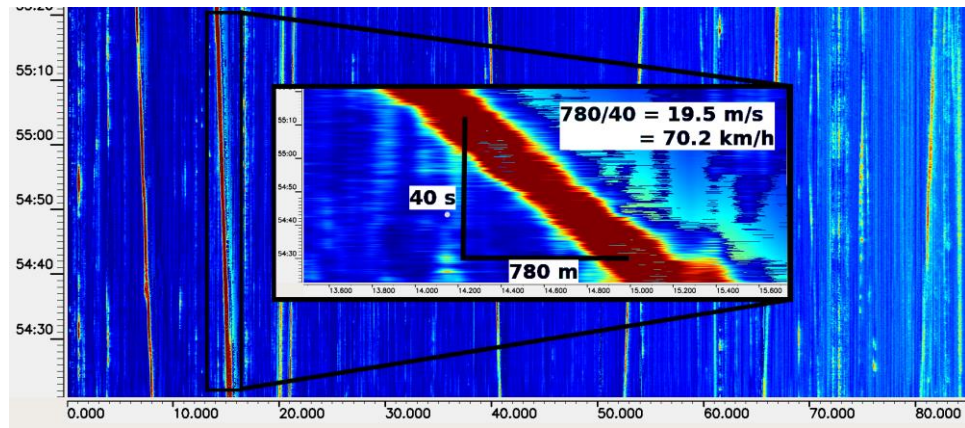
**Figure 21**. The waterfall with moving vibration sources (trains) and the source movement speed estimation

When the sensing cable is laid down along the railway line the train speed profile can be obtained as shown in **Figure 22**. Thus the system can provide useful information if needed.

**Figure 22**. The speed profile of the train and its map location at selected time instant

Not only strong vibration sources can be detected and localized at far distance but also a human or bigger animal presence in the vicinity of the sensing fiber are reported by the sensing system, see **Figure 23**. The optic pulse power was 23 dBm and pulses width was 1μs. The sensing cable was a standard SM telecom cable laid approximately 1 m under the ground surface. It can be seen that the signal influenced by the running person is clearly detectable including the direction of movement.
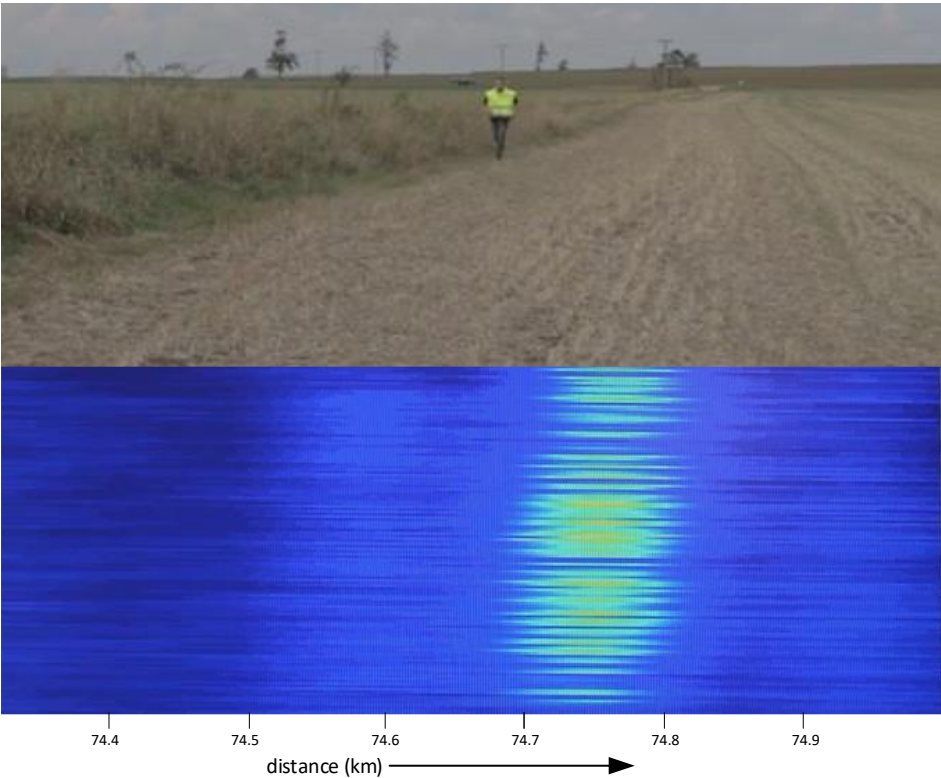
**Figure 23**. Detection of runing person at the distance 74.75 km

### 2.1. Two-fiber sensor unit design

The two-fiber sensor unit designed according to the scheme depicted in **Figure 10** was also constructed and tested. The system testing was accomplished in the laboratory. The system is working correctly as shown in **Figure 24**. Two fiber coils, 50 km each, were used as sensing traces. Both pictures **Figure 24** a) and **Figure 24** b) shows that the ends of both fibers are clearly detectable.

a)

b)

c)
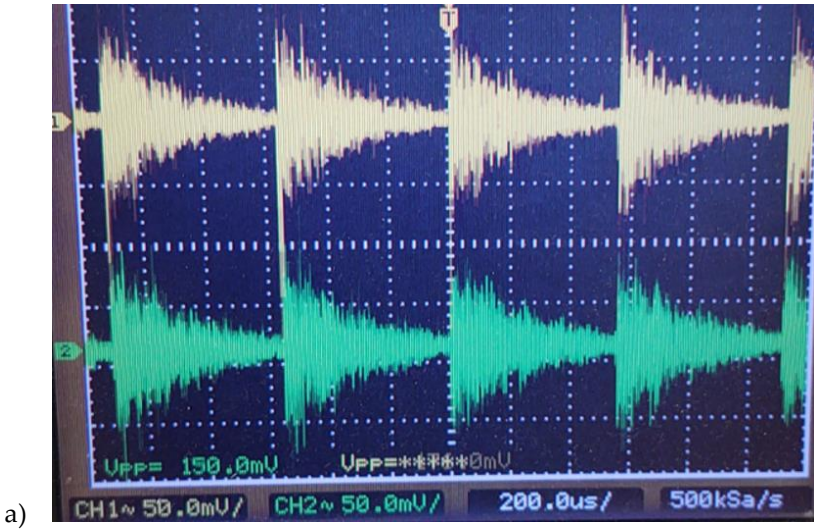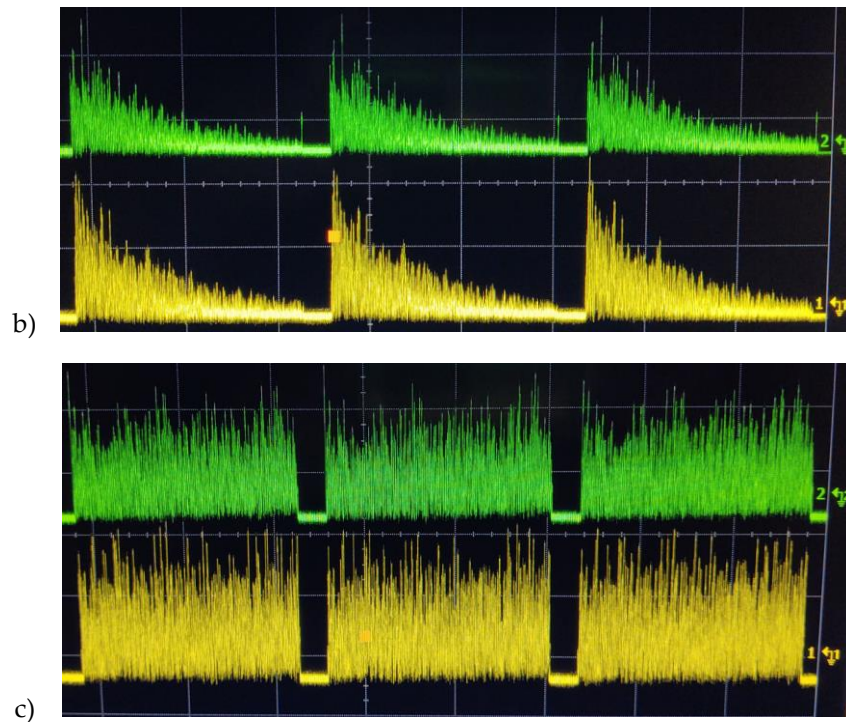
**Figure 24**. Two-fiber sensor signals obtained from two 50 km links: a) signals at the outputs of o/e convertors, b) signals after mixing and low-pass fitering without equalization, c) equalized traces ready for A/D conversion

Raw waterfalls (before other processing) from both sensing fibers can be seen in **Figure 25**. It is evident from the vertical time axis scale that the system is in a stable state for more than 10 second intervals even if the sensing fiber is a coiled bare fiber with 250 µm primary coating only.
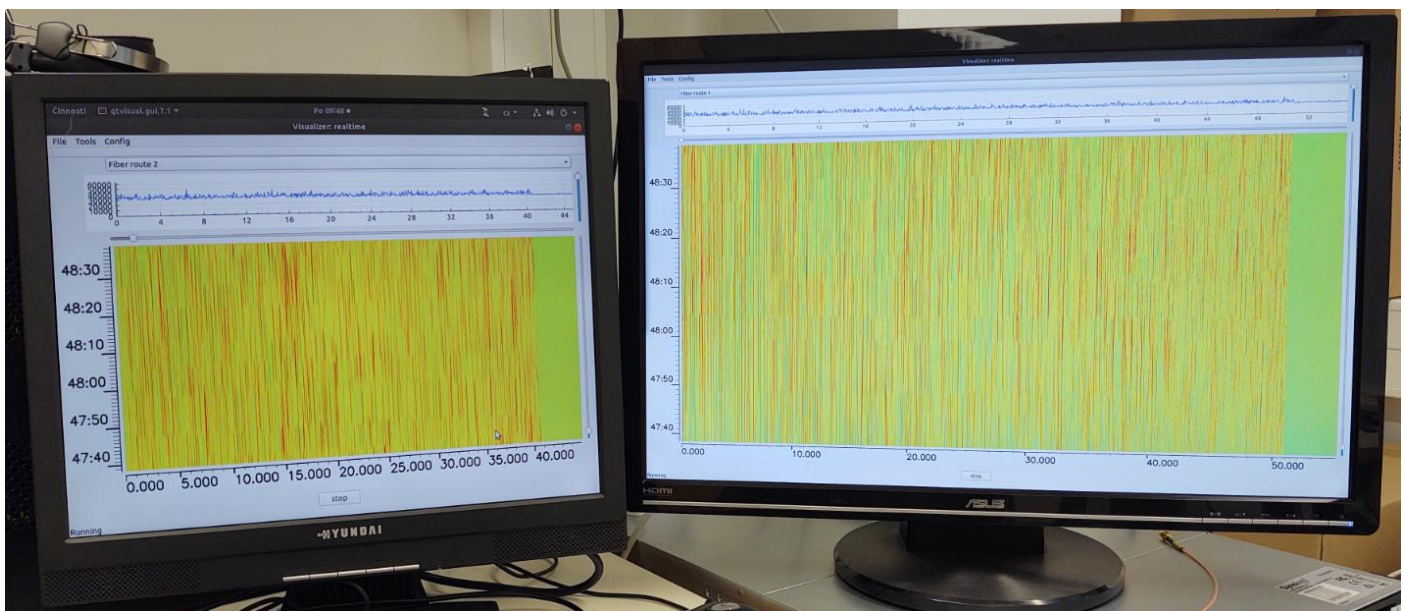
**Figure 25**. Raw waterfalls from the two fibers – 40 and 50 km long

The ready sensor unit consisting of interrogation and computer modules and shown in **Figure 26** was tested a few weeks ago in a real set up. The test sensing trace contains Mini LT Flat Drop 09/125 cable directly buried under ground. Two fibers of the cable were connected to the system simultaneously. The graphical user interface is a separate application that can run remotely as shown in **Figure 26** b).

a)                                                                                                                        b)
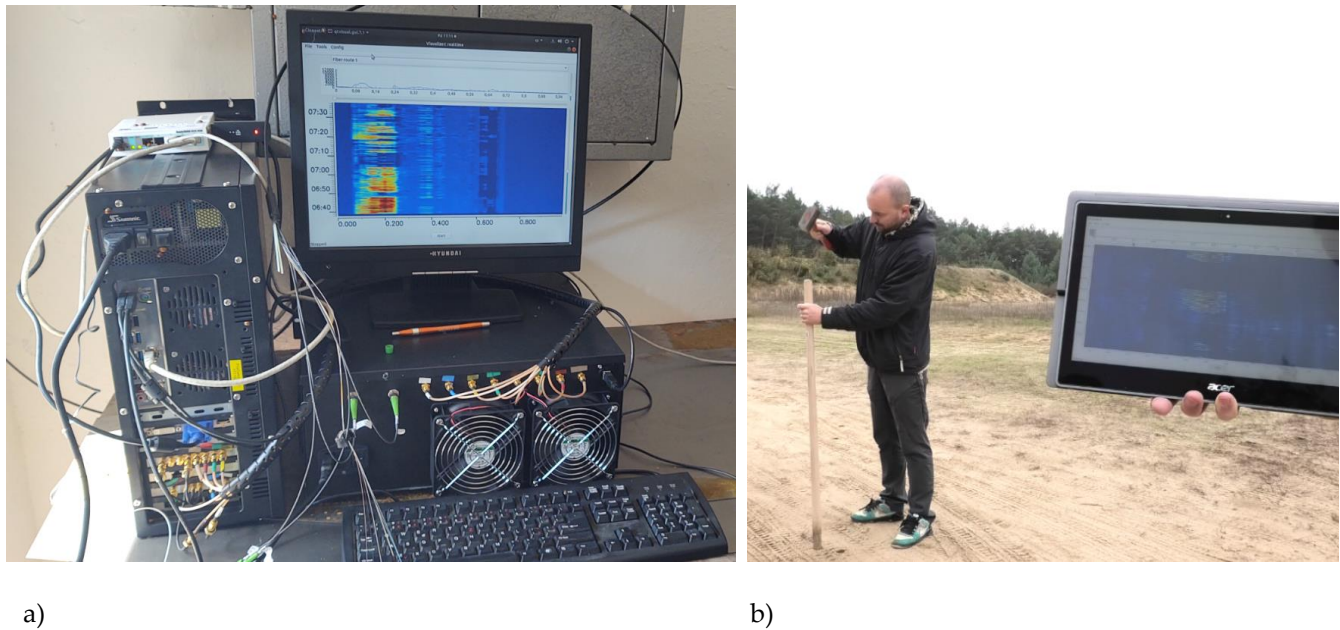
**Figure 26**. Two-fiber system testing under real conditions: a) the sensing unit; b) the generation of vibrations and the measurement remote control

A good quality mobile data connection (several Mbps capacity) is required to control and to watch the waterfall. A number of different events generating mechanical vibrations (rod hammering, ground digging, person walk and run, car movement, etc.) were generated and a lot of data were collected for event classifier machine learning process.

## 3. Discussion

The distributed vibration sensing system based on Rayleigh backscattering and on the coherent detection principle was designed and constructed. It is capable to detect and to localize many vibration sources, both static and moving ones. Maximum sensing length reachable by our single fiber system is above 90 km and more than 150 km with two-fiber sensor unit. Implementing the additional signal processing our system can also identify several groups of vibration sources – trains, cars, persons (jumping, walking, running), ground digging, drilling, hammering. These days we have been finishing a two-fiber sensor unit. Described sensing units are the parts of a more complex sensing system, which we designed, and which has been tested since the end of last year and which is described in [27]. The system is scalable, i.e. it can run more sensing units concurrently and for more independent customers, whose receive required information through a security gateway.

**Author Contributions:** System architecture, methodology, Novotny, V.; hardware design Novotny, V., Hanak, P., Prokes, A.; software, Sysel, P., Prinosil, J.; system validation, Novotny, V., Sysel, P., Slavicek, K.; investigation, Novotny, V.; data processing, Sysel, P., Prinosil, J.; writing, Novotny, V., Sysel, P., Slavicek, K. visualization, Sysel, P.; supervision Novotny, V.; project administration, Novotny, V.; funding acquisition, Novotny, V.

**Funding:** This research was funded by Ministry of Interior of the Czech Republic under grant no. VI20172020078.

**Conflicts of Interest:** The authors declare no conflict of interest.

## 4. References

1.  Bhavin J. S. and Plant, D. V. Scaling Technologies for Terabit Fiber Optic Transmission. *Proc. of SPIE, Optoelectronic Integrated Circuits XIII*, Vol. 7942, pp. 1-12, 2011, doi:10.1117/12.880247

2.  Eric U. W.; Spillman B. Jr. *Fiber Optic Sensors: An Introduction for Engineers and Scientists* (Second edition). John Wiley & Sons, ISBN 978-0-470-1264-4, New Jersey, USA, 2011

3.   Quan Chai, Yang Luo, Jing Ren, Jianzhong Zhang, Jun Yang, Libo Yuan, Gangding Peng, "Review on fiber-optic sensing in health monitoring of power grids," *Opt. Eng*. 58(7) 072007 (26 February 2019) https://doi.org/10.1117/1.OE.58.7.072007

4.   Fernandez-Ruiz, María R., Marcelo A. Soto, Ethan F. Williams, Sonia Martin-Lopez, Zhongwen Zhan, Miguel Gonzales-Herralez and Hugo F. Martins. Distributed acoustic sensing for seismic activity monitoring. *APL Photonics* [online]. 2020, 5(3). ISSN 2378-0967. Available at: doi:10.1063/1.5139602

5.   Wiesmyr, Christoph, Martin Litzenberg, Markus Waser, Adam Papp, Heinrich Garn, Günther Neunteufel a Herbert Döller. Real-Time Train Tracking from Distributed Acoustic Sensing Data. *Applied Sciences* [online]. 2020, 10(2). ISSN 2076-3417. Available at: doi:10.3390/app10020448

6.   Barrias, António, Joan Casas a Sergi Villalba. A Review of Distributed Optical Fiber Sensors for Civil Engineering Applications. *Sensors* [online]. 2016, 16(5) [cit. 2021-5-16]. ISSN 1424-8220. Available at: doi:10.3390/s16050748

7.   Wrobel, J. at all. Analysis of Temperature Dependence of Dark Current Mechanisms in Mid-Wavelength Infrared pin Type-II Superlattice Photodiodes. *Sensors and Materials*, Vol. 26, No. 4 (2014) 235–244, MYU Tokyo, 2014

8.   Byeong H. L.; Young H. K.; Kwan S. P.; Joo B. E.; Myoung J. K.; Byung S. R. and Hae Y. Ch. Interferometric Fiber Optic Sensors. *Sensors*, ISSN 1424-8220, pp. 2467-2486, 2012

9.   Thénevaz, L. *Brillouin distributed time-domain sensing in optical fibers: state of the art and perspectives* [online]. Higher Education Press and Springer-Verlag Berlin Heidelberg 2010 URL: http://infoscience.epfl.ch/record/143879

10.  Maughan, S. M. *Distributed Fiber Sensing Using Microwave Heterodyne Detection of Spontaneous Brillouin Backscatter* (Doctoral thesis). University of Southampton, 2001, UK.

11.  Martins, Hugo F., Sonia Martin/Lopez, Pedro Corredera, Massimo L. Filograno, Orlando Frazao a Miguel Gonzalez-Herraez. Phase-sensitive Optical Time Domain Reflectometer Assisted by First-order Raman Amplification for Distributed Vibration Sensing Over >100 km. *Journal of Lightwave Technology* [online]. 2014, 32(8), 1510-1518 [cit. 2021-5-17]. ISSN 0733-8724. Dostupné z: doi:10.1109/JLT.2014.2308354

12.  Detection Performance Improvement of Distributed Vibration Sensor Based on Curvelet Denoising Method. *Sensors* [online]. 2017, 17(6). ISSN 1424-8220. Available at: doi:10.3390/s17061380

13.  Meiqi, R. *Distributed Optical Fiber Vibration Sensor Based on Phase-Sensitive Optical Time Domain Reflectometry*. MS.C. thesis at University of Ottawa, 2016.

14.  Xiong, Ji, Zinan Wang, Yue Wu a Yunjiang Rao. Single-Shot COTDR Using Sub-Chirped-Pulse Extraction Algorithm for Distributed Strain Sensing. *Journal of Lightwave Technology* [online]. 2020, 38(7), 2028-2036. ISSN 0733-8724. Available at: doi:10.1109/JLT.2020.2968632

15.  McCarron, D. J. *A Guide to Acousto-Optic Modulators*. http://massey.dur.ac.uk/resources/slcornish/AOMGuide.pdf, 2007

16.  *AA Opto-Electronic Acousto-Optic Theory*. 2013, http://www.aaoptoelectronic.com/Documents/AAOPTO-Theory2013-4.pdf, ref. 05/2016

17.  Redding, Brandon, Matthew J. Murray, Allen Davis a Clay Kirkendall. Quantitative amplitude measuring φ-OTDR using multiple uncorrelated Rayleigh backscattering realizations. *Optics Express* [online]. 2019, 27(24). ISSN 1094-4087. Available at: doi:10.1364/OE.27.034952

18.  Wang, Zinan, Li Zhang, Song Wang, et al. Coherent Φ-OTDR based on I/Q demodulation and homodyne detection. *Optics Express* [online]. 2016, 24(2). ISSN 1094-4087. Available at: doi:10.1364/OE.24.000853

19.  Liehr S, Muanenda YS, Münzenberger S, Krebber K. Relative change measurement of physical quantities using dual-wavelength coherent OTDR. *Opt Express*. 2017 Jan 23;25(2):720-729. doi: 10.1364/OE.25.000720. PMID: 28157961.

20.  He, H.; Shao, L.-Y.; Li, Z.; Zhang, Z.; Zou, X.; Luo, B.; Pan, W.; Yan, L. Self-Mixing Demodulation for Coherent Phase-Sensitive OTDR System. *Sensors* 2016, *16*, 681. https://doi.org/10.3390/s16050681

21.  Liu, Xin, Baoquan Jin, Qing Bai, Yu Wang, Dong Wang a Yuncai Wang. Distributed Fiber-Optic Sensors for Vibration Detection. *Sensors* [online]. 2016, 16(8). ISSN 1424-8220. Available at: doi:10.3390/s16081164

22.  Bao, Xiaoyi, Da-Peng Zhou, Chams Baker a Liang Chen. Recent Development in the Distributed Fiber Optic Acoustic and Ultrasonic Detection. *Journal of Lightwave Technology* [online]. 2017, 35(16), 3256-3267. ISSN 0733-8724. Available at: doi:10.1109/JLT.2016.2612060

23.  Zinsou, Romain, Xin Liu, Yu Wang, Jianguo Zhang, Yuncai Wang a Baoquan Jin. Recent Progress in the Performance Enhancement of Phase-Sensitive OTDR Vibration Sensing Systems. *Sensors* [online]. 2019, 19(7). ISSN 1424-8220. Available at: doi:10.3390/s19071709

24.  Wang, Z.; Lu, B..; Ye, Q. and Cai, H. Recent Progress in Distributed Fiber Acoustic Sensing with Φ-OTDR. *Sensors* [online]. 2020, ISSN 1424-8220. Available at: doi:10.3390/s20226594

25.  Novotny V. (2018) Enhancement of Distributed Fiber Optic Vibration Sensors. In: Duy V., Dao T., Zelinka I., Kim S., Phuong T. (eds) *AETA 2017 - Recent Advances in Electrical Engineering and Related Sciences: Theory and Application*. AETA 2017. *Lecture Notes in Electrical Engineering*, vol 465. Springer, Cham. https://doi.org/10.1007/978-3-319-69814-4_20

26.  Novotny, V.; Sysel, P. Long-Range Optical Fibre Based Distributed Vibration Sensing. The *KTTO 2016 conference proceedings*, 2016, 6 pp, p. 38-43. ISBN: 978-80-248-3959- 2.

27.  Novotny, V.; Sysel, P.; Prinosil, J.; Mekyska, J.; Slavicek, K. and Lattenberg, I. Critical Infrastructure Monitoring System. In: *2021 IEEE 17th International Colloquium on Signal Processing & Its Applications (CSPA)* [online]. IEEE, 2021, 2021-3-5, s. 165-170. ISBN 978-1-6654-1484-5. doi: 10.1109/CSPA52141.2021.9377303